

MODELING A HYBRID BEAM-COLUMN CONNECTION IN PRECAST RC STRUCTURES

Mosab Yaghoubi, MS student, Dept. of Civil Engineering, Kharazmi University, Tehran, Iran; Mosab.Yaghobi@gmail.com

Ali Massumi, PhD, Dept. of Civil Engineering, Kharazmi University, Tehran, Iran

Farhang Farahbod, PhD, Road, Housing & Urban Development Research Center, Tehran, Iran

ABSTRACT

Precast concrete elements in buildings offers benefits such as cost-effectiveness, and speed and ease of erection. Experimental testing on precast structural systems under simulated seismic loading has demonstrated that an unbounded, post-tensioned (hybrid) frame, if well-designed and constructed, performs as a ductile connection for equivalent monolithic systems. The important feature of this system is the elimination of residual drift after an earthquake. The seismic performance of hybrid beam-column connections in precast structural systems can improve the behavior of this connection. This study used experimental testing results from previous research by NIST to develop a finite element computer program model. The results showed good correlation between numerical analysis and the experimental results and it can be concluded that this model is reliable to be used in future researches.

Keywords: Precast, Unbounded, Post-tensioned, Hybrid, Finite element

INTRODUCTION

Previous earthquakes, such as those in Armenia (1988), Kobe, Japan (1995), and Kocaeli, Turkey (1999)¹, have shown that the beam-column connections in precast structures play an important role in seismic behavior. Post-tensioning is a convenient method for connecting precast concrete elements. Precast concrete elements can be made into continuous structures using post-tensioned tendons. This study surveys well-established and less common innovative solutions, including hybrid systems, where unbonded post-tensioned tendons in combination with mild steel are used to assemble elements to minimize residual drift. The term hybrid signifies response behavior between non-linear elastic and elasto-plastic. It maintains the re-centering properties of the former and the variable dissipative properties of the latter¹.

Most pre-stressed concrete buildings today are constructed by assembling precast units by post-tensioning¹. Experimental tests have improved the behavior of precast beam-column connections. This study developed a 3D model of a connection using ANSYS release 14 finite element program. The model was subjected to reverse cyclic loading in accordance with a prescribed displacement history.

EXPERIMENTAL DATA

Most experimental data was extracted from research done by Choek and Stone² and Hawileh et al.¹⁰. Cheok and Stone² conducted experimental tests at the National Institute of Standards and Technology (NIST). The present study modeled the M-P-Z4 specimen using phase IV of the Precast Seismic Structural Systems (PRESSSS) program.

The connections are termed hybrid because they contain both mild or low strength steel and prestressed (PT) or high strength steel. Hybrid connections composed of mild steel was used as energy dissipaters located at the top and bottom of a beam. Post-tensioned steel was located at the centroid of the beam. The friction force developed between the beam and the column by the post-tensioning force provides the necessary shear resistance. The mild steel was deboned 25 mm on either side of the beam-column interface to delay fracture of the bars². Geometry and section details are shown in Figs. 1 and 2².

MATERIAL PROPERTIES

CONCRETE

Development of a model for the behavior of concrete is a challenging task. Concrete is a quasi-brittle material and exhibits different behaviors in compression and tension. The tensile strength of concrete is typically 8-15% of the compressive strength³. Fig. 3 shows a typical stress-strain curve for normal weight concrete⁴. Material properties of concrete are illustrated in Table 1.

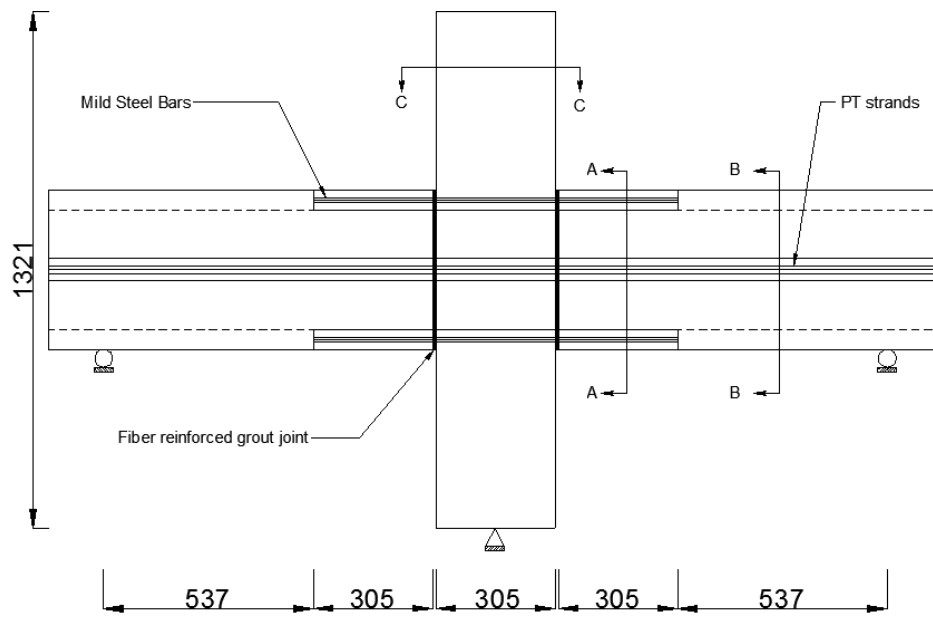


Fig. 1. Geometry of the M-P-Z4 model² (mm).

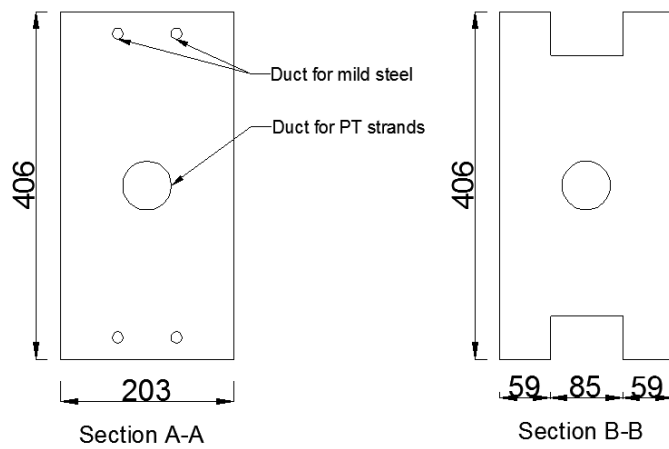


Fig. 2. Section details of M-P-Z4² (mm).

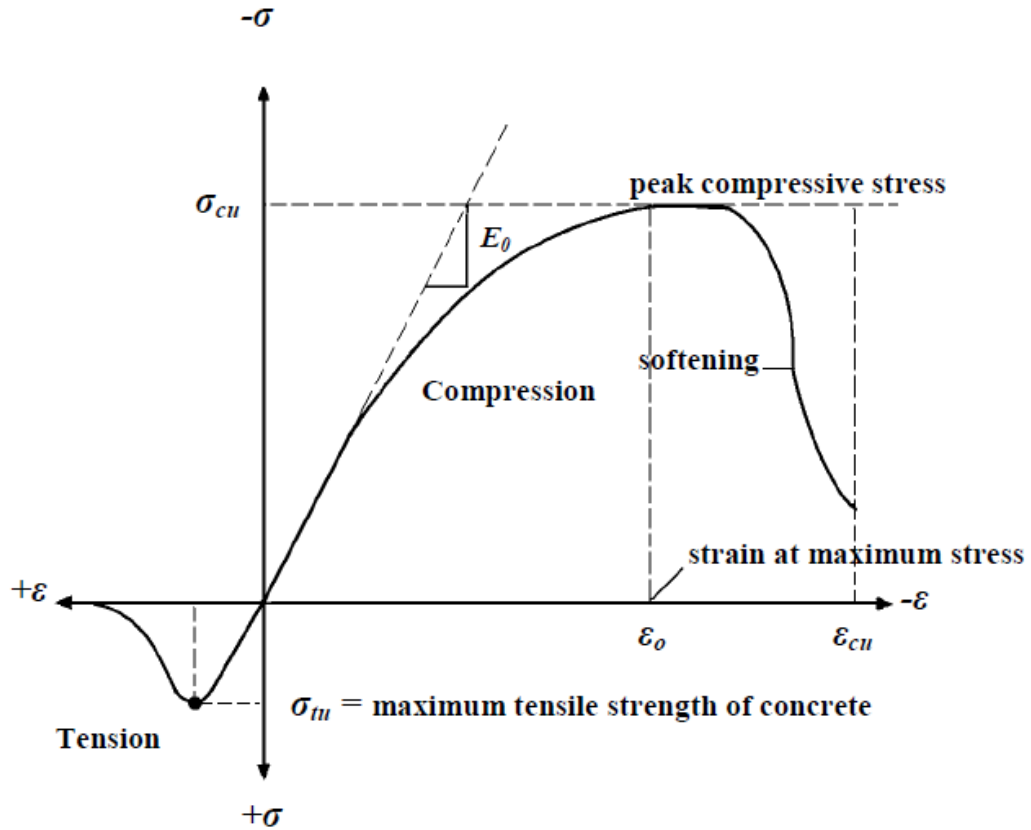


Fig. 3. Typical uniaxial compressive and tensile stress-strain curve for concrete⁴.

Table 1. Concrete properties^{2,10}.

Concrete Material	f _c (MPa)	E (MPa)	f _r (MPa)
Beam and column concrete	51	31000	3.45
Interface grout	76	23800	4.14

The ANSYS program requires a uniaxial stress-strain relationship for concrete in compression. The numerical expressions⁵ in Equations (1) and (2) were used with Equation (3) to construct a uniaxial compressive stress-strain curve for concrete⁶:

$$f = \frac{E_c \varepsilon}{1 + \frac{\varepsilon}{\varepsilon_0}} \quad (1)$$

$$\varepsilon_0 = \frac{2f'_c}{E_c} \quad (2)$$

$$E_c = \frac{f}{\varepsilon} \quad (3)$$

where:

f = stress at any strain ε

ε = strain at stress f

ε_0 = strain at the ultimate compressive strength f'_c

FAILURE CRITERIA OF CONCRETE

The model is capable of predicting failure for concrete materials and accounts for both cracking and crushing failure modes. Two input strength parameters, ultimate uniaxial tensile and compressive strengths, are needed to define a failure surface for the concrete. Using them, a criterion for failure of the concrete caused by a multiaxial stress state can be calculated⁷.

The model of 3D failure surface for concrete is shown in Fig. 4 for states of stress that are biaxial or nearly biaxial. If the most significant nonzero principal stresses are in the σ_{xp} and σ_{yp} directions, the three surfaces presented are for an σ_{zp} of slightly greater than zero, σ_{zp} equal to zero, and σ_{zp} slightly less than zero. Although the three surfaces shown as projections on the $\sigma_{xp} - \sigma_{yp}$ plane are nearly equivalent and the 3D failure surface is continuous, the mode of material failure is a function of the sign of σ_{zp} . For example, if σ_{xp} and σ_{yp} are both negative and σ_{zp} is slightly positive, cracking can be predicted in a direction perpendicular to the σ_{zp} direction; however, if σ_{zp} is zero or slightly negative, the material is assumed to be crushed⁹.

A pure compression failure of concrete is unlikely. In a compression test, the specimen is subjected to a uniaxial compressive load. Secondary tensile strains induced by the Poisson effect occur perpendicular to the load. Because concrete is relatively weak in tension, these actually cause cracking and eventual failure^{8,3}. In this study, the crushing capability was turned off and cracking of the concrete controlled the failure of the finite element models.

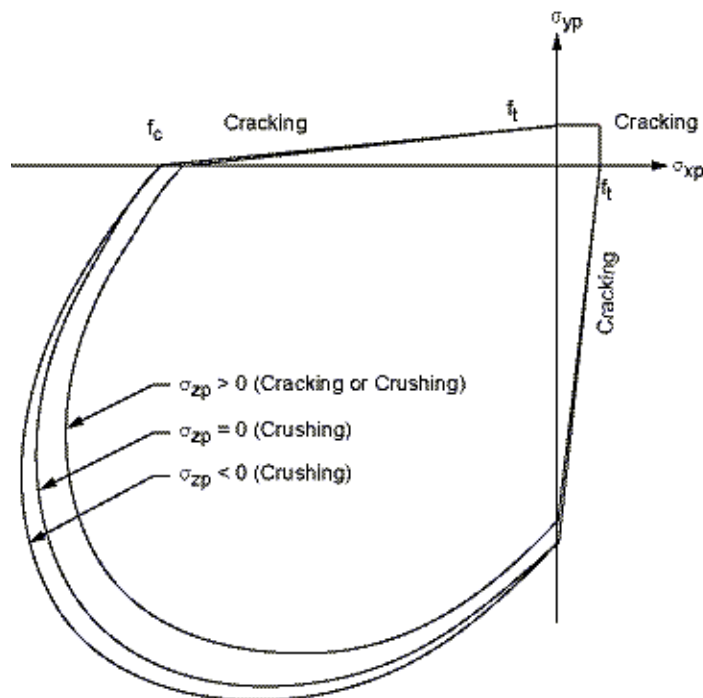


Fig. 4. Failure surface in principal stress space with nearly biaxial stress⁹.

STEEL

All stirrups in the beams and ties in the column were welded reinforcement grids. The specimen was post-tensioned with 3-13 mm grade 270 prestressing strands located at the beam centroid. The M-P-Z4 specimen was two (top and bottom) #3 mild steel grade 60 reinforcing bars ($f_{py} = 414 \text{ MPa}$)². The steel material properties are shown in **Error! Reference source not found. 2**.

Table 2. Properties of steel material².

Steel material properties	E (MPa)	f_y (MPa)
mild steel bars (grade 60)	2.00E+05	414
beam and column stirrup	2.00E+05	600
beam reinforcing bars	2.00E+05	520
column reinforcing bars	2.00E+05	414
prestressing tendon (grade 270)	2.00E+05	$f_u = 1862$

ASSIGNED ELEMENTS

CONCRETE

An 8-node solid element, SOLID65, was used to model the concrete. The 8 nodes have 3 degrees of freedom at each node translation in the nodal x , y , and z directions. The element is capable of plastic deformation, cracking in 3 orthogonal directions, and crushing.

The solid capability of the element can be used to model the concrete and the rebar capability can be used to model reinforcement behavior. The solid is capable of cracking in tension and crushing in compression, but, as mentioned, the crushing capability of the concrete element was turned off to aid convergence. The geometry, node locations, and coordinate system for this element are shown in Fig. 5.

REBARS

All stirrups in the beams and the ties in the column were modeled with rebar capability in SOLID65 elements, but the main reinforcement of the beams and column and mild steel bars were modeled as LINK180 elements. A LINK180 element is a uniaxial tension-compression element with 3 degrees of freedom at each node and translations in the nodal x , y , and z directions. As in a pin-jointed structure, no bending of the element is considered. Plasticity, creep, rotation, large deflection, and large strain capabilities are included⁹. The geometry and node locations for this element type are shown in Fig. 6.

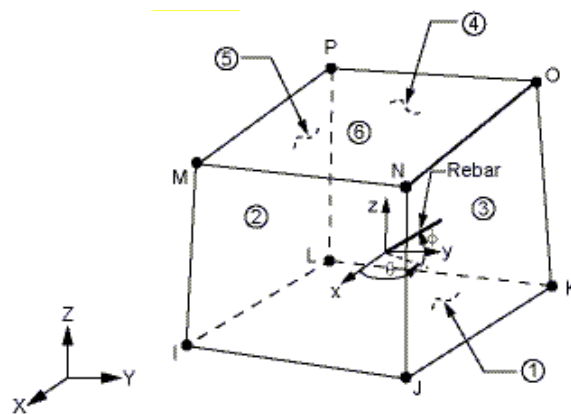


Fig. 5. SOLID65 geometry⁹.

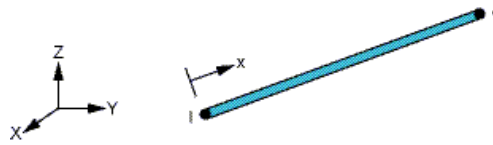


Fig. 6. LINK180 geometry⁹.

POST-TENSION TENDON

SOLID185 was used to model the post-tensioned cable because it allows for prism, tetrahedral, and pyramid degenerations when used in irregular regions⁹. The geometry and node locations for this element type are shown in Fig. 7.

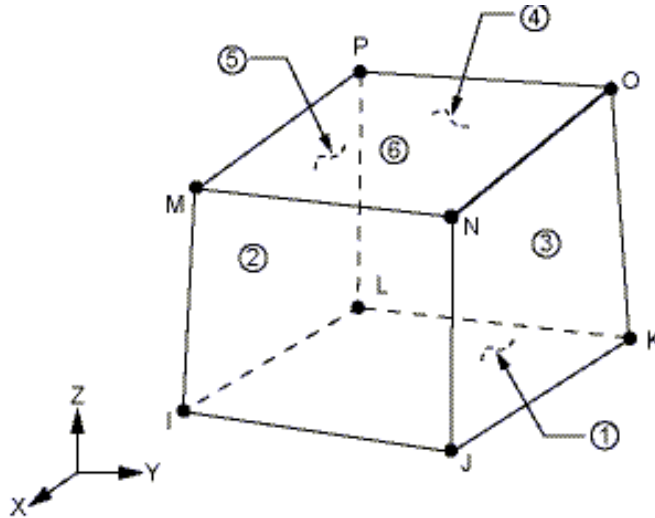


Fig. 7. SOLID185 homogeneous structural solid geometry⁹.

CONTACT ELEMENT

Surface-to-surface contact elements (CONTACT174 and TARG170) with a friction coefficient of 0.5 were used between the beam, interface grout and column. It should be noted that the duct grout was not modeled, so no contact was modeled between the post-tensioned tendon and the concrete through the duct hole. The ends of the tendon were only coupled with the beam end nodes. Penetration tolerance was increased to 0.5 in response to the “too much penetration” error from the program that may have been a result of the pre-stressed condition.

FINITE ELEMENT MODELING POINTS

- The 3D finite element model was analyzed under cyclic loading using the nonlinear static analysis method.
- The areas of the 3 experimental post-tensioning cables were held equal to model a cylindrical SOLID185 as a post-tensioning cable.
- In the experimental test, the mild steel was deboned 25 mm on either side of the beam-column interface to delay fracture of the bars². To model this condition, the SOLID65 nodes were not connected to the LINK180 element at this length.
- The post-tension tendon was bonded at a length equal to 1/3 of the tendon length², but this condition was not modeled in this study.
- The experimental test showed that the fracture of mild steel bars resulted in the failure of specimen M-P-Z4². Reinforcement was modeled using LINK 180 to assure that no slippage took place between the concrete nodes and the mild steel bars.
- The total number of elements was 11137.

BOUNDARY CONDITIONS

The boundary conditions for the connection are shown in Fig. 8 and, for the test specimen, were as follows: pinned at the column bottom and roller supported at the column top and beam ends². Historical loading was applied to the top of the column. The basic loading history is 3 cycles at a specific drift level². In this study, only one cycle at each drift was level applied to the connection.

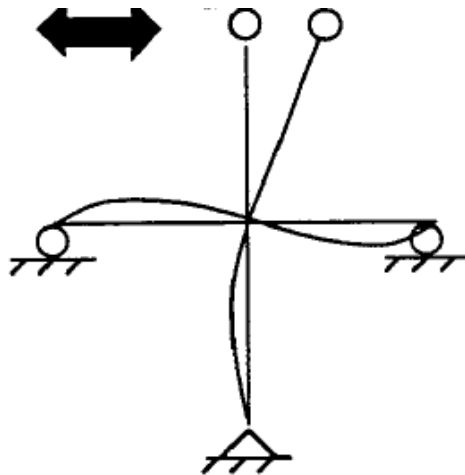


Fig. 8. Boundary conditions for the connection².

The initial stresses in the prestressing strands were approximately equal to 827 MPa or $0.44 f_{pu}$ ² and to 247kN applied to the tendons solid (SOLID185 elements). As mentioned, a

load of approximately 20 kN was applied in the experimental data to each beam approximately 89 mm from the column face². In the finite element model, it was applied at 85 mm. An axial load equal to 1200 kN was applied to the top face of the column¹⁰ by modeling 12.9 MPa of pressure to the column element.

Cyclic loads were applied to a node at the top of the column as a master node. To avoid stress concentration and to obtain the reaction results more easily, a line node from the top of the column in the x direction were coupled with the master node.

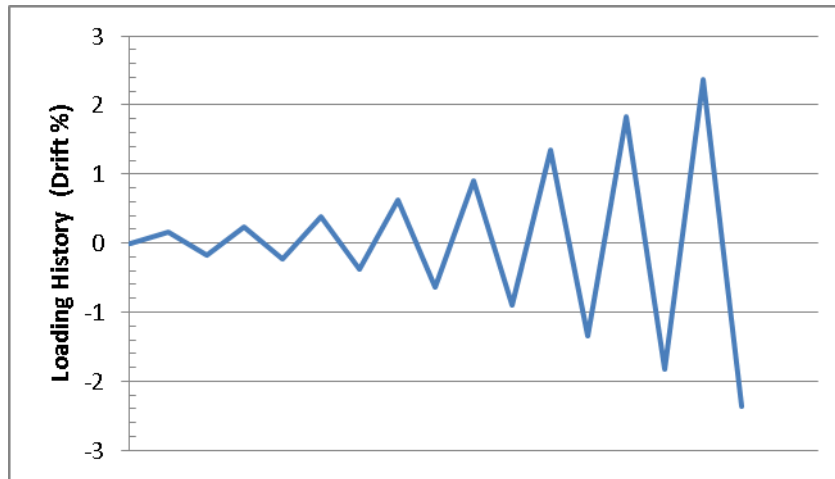


Fig. 9. Basic loading history for the specimen².

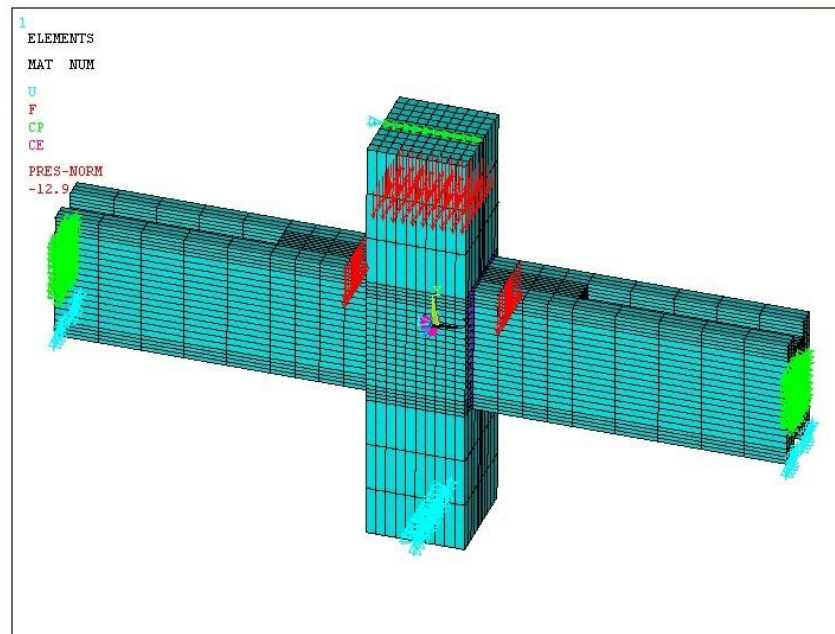


Fig. 10. Model meshing.

RESULTS AND CONCLUSION

- Fig. 11 shows the finite element hysteresis vs. experimental curves. Good correlation was observed. The peak load from finite element analysis shows approximately 11% more than the experimental in the last loop of the hysteresis curves.

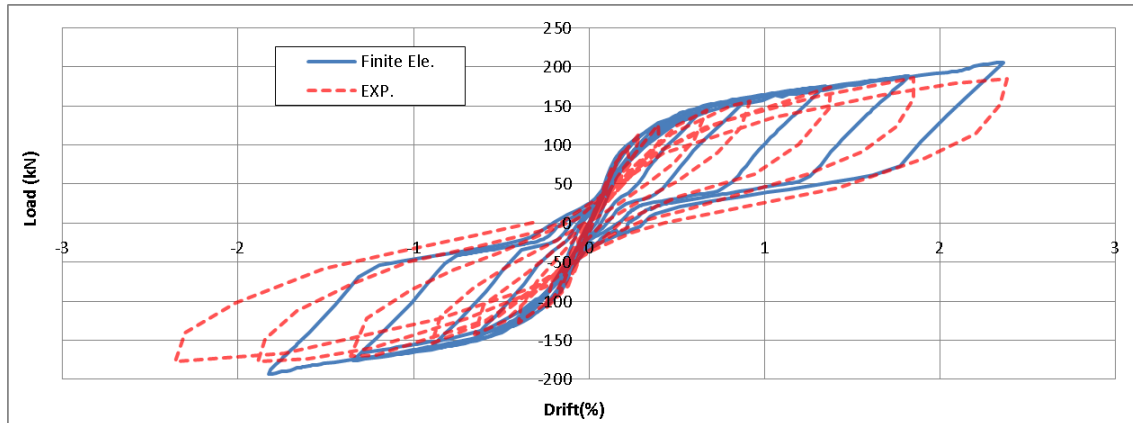


Fig. 11. Hysteresis curves for finite element analysis and experimental² data.

- As mentioned, in Cheok and Stone², no slip of the beam related to the column was observed during finite element analysis.
- The post-tensioned tendon remained elastic during finite element analysis and is in scope of the experimental test².

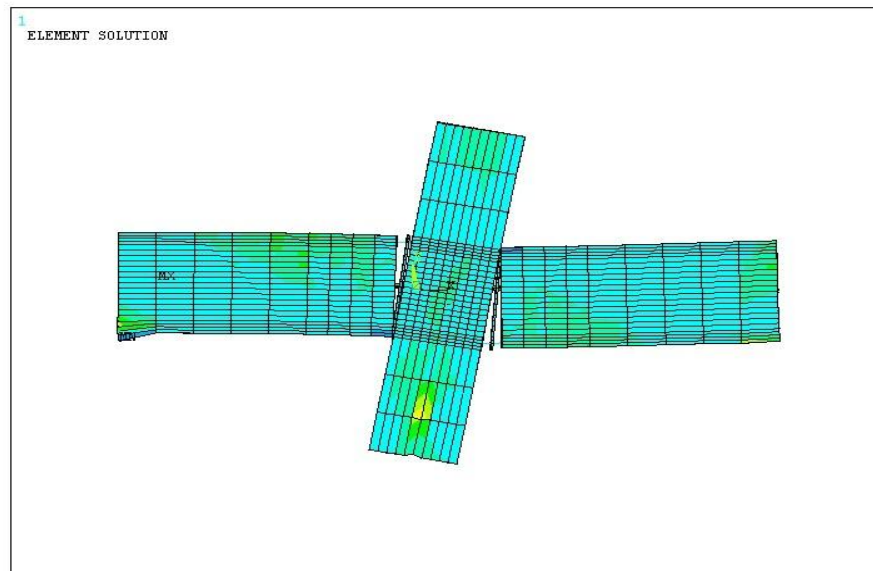


Fig. 12. Deformed shape with enlarging scale factor.

REFERENCES

1. Park, R, “Seismic Design of Precast Concrete Building Structures: State-of-Art Report Prepared by Task Group 7.3, Fédération International du Béton, 2003.
2. Cheok, G.S. and Stone, W.C., “Performance of 1/3 Scale Model Precast Concrete Beam–Column Connections Subjected to Cyclic Inelastic Loads”, Report No. NISTIR 5436, NIST, Gaithersburg, MD, 1994.
3. Shah, S.P., Swartz, S.E., and Ouyang, C., *Fracture Mechanics of Concrete*, John Wiley & Sons, Inc., New York, NY, 1995.
4. Bangash, M.Y.H., *Concrete and Concrete Structures: Numerical Modeling and Applications*, Elsevier Science Publishers Ltd., London, England, 1989.
5. Desayi, P. and Krishnan, S., “Equation for the Stress-Strain Curve of Concrete,” *Journal of the American Concrete Institute*, V. 61, March 1964, pp. 345-350.
6. Gere, J.M. and Timoshenko, S.P., *Mechanics of Materials*, PWS Publishing Co., Boston, MA, 1997.
7. William, K.J. and Warnke, E.P., “Constitutive Model for the Triaxial Behavior of Concrete: Proceedings of the International Association for Bridge and Structural Engineering”, V. 19, ISMES, Bergamo, Italy, 1975, pp. 174.
8. Mindess, S. and Young, J.F., *Concrete*, Prentice-Hall, Inc., Englewood Cliffs, NJ, 1981.
9. ANSYS Release 14.0 Help, 2011
10. Hawileh, R.A. Rahman, A., and Tabatabai, H., “Nonlinear Finite Element Analysis and Modeling of a Precast Hybrid Beam–Column Connection Subjected to Cyclic Loads”, *Applied Mathematical Modelling*, V. 34, 2010, pp. 2562–2583